JACS
JOURNAL OF THE AMERICAN CHEMICAL SOCIETY

Communication

pubs.acs.org/JACS

# Spin-Reconstructed Proton-Coupled Electron Transfer in a Ferrocene–Nickeladithiolene Hybrid

Akira Tanushi, Tetsuro Kusamoto,* Yohei Hattori, Kenji Takada, and Hiroshi Nishihara*

Department of Chemistry, Graduate School of Science, The University of Tokyo, 7-3-1 Hongo, Bunkyo-ku, Tokyo 113-0033, Japan

Supporting Information

**ABSTRACT:** A proton–electron dual-responsive system based on a hybrid of ferrocene and metalladithiolene (**1**) was developed. The formation of the dithiafulvenium moiety was driven by protonation of the metalladithiolene unit of **1** and by oxidation. The change in the electronic structure caused by the protonation was combined with the redox properties of the two components of **1**, generating two radical species with different spin density distributions (3d spin and $\pi$ spin). Furthermore, a spin-reconstructed proton-coupled electron transfer, i.e., the transformation from 3d spin to $\pi$ spin accompanied by deprotonation, was achieved by a temperature change, the third external stimulus.

Multifunctionality of a single molecule controlled by multiple external stimuli has attracted attention in basic and applied science, as the interplay between the functions can result in unique properties and novel molecule-based materials.[1] A promising strategy for developing these systems is to incorporate stimuli-responsive properties such as a proton-responsive ability into redox-active (i.e., electron-responsive) molecules, as seen in proton-coupled electron transfer (PCET) systems.[2] Of particular interest developed in this field is PCET accompanied by a large reconstruction of the spin density distribution, termed spin-reconstructed PCET (SR-PCET).[3] The spin reconstruction driven by PCET gives rise to drastic changes in the magnetic and conducting properties and electronic structure of the system. To date, SR-PCET has been achieved within dimeric molecules, and there have been only a limited number of reports. Therefore, investigations of spin reconstruction within single molecules are important to expand the scope of this phenomenon for use in single-molecule spintronic devices.[4]

Many metalladithiolenes show multistep redox activities coupled with $\pi$-conjugated characteristics, which allow for the development of interesting electron-transfer properties.[5] We have prepared metalladithiolenes functionalized with 2,2,6,6-tetramethylpiperidine-1-oxyl (TEMPO) or ferrocene (Fc). They exhibit interesting electronic structures and functions such as SOMO–HOMO level conversion and reversed intramolecular charge transfer.[6] Appropriate connection of the functional moieties to the metalladithiolene framework produces unique electronic structures and properties based on the intrinsic redox activity of metalladithiolenes.

In this study, we aimed to develop novel SR-PCET phenomena on a single molecule by introducing a proton-responsive property into the electron-responsive metalladithiolene system. Among several chemical structures that act as proton-responsive sites (e.g., the pyridine skeleton),[7] we focused on the dithiafulvene skeleton in our metalladithiolene framework. The dithiafulvene skeleton forms dithiafulvenium upon oxidation, accompanied by quasi-aromatization of the five-membered ring (Scheme 1a). We expected that the quasi-aromatization would also be driven by protonation at the double bond proximal to the dithiafulvene skeleton, giving rise to a large modulation of the molecular and electronic structures (Scheme 1a).

**Scheme 1. (a) Oxidation and Protonation of a Dithiafulvene Unit; (b) Proton- and Electron-Responsive Properties Based on Ni(dppe)($FcS_4dt$)**

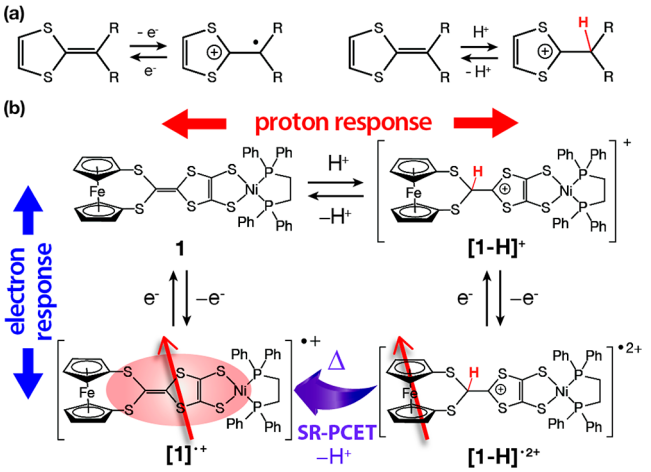


Herein we report the proton–electron dual-responsive properties of Ni(dppe)($FcS_4dt$) (**1**), a hybrid of Fc and nickeladithiolene. The interplay of the two stimuli-responsive characteristics generates two radical species with different spin density distributions (3d spin and $\pi$ spin). **1** displays temperature-gated SR-PCET on a single-molecule level with a dramatic transformation of the spin characteristics from 3d spin to $\pi$ spin (Scheme 1b).

**1** was prepared by a modified version of a method described in the literature[6c] and characterized by $^1$H NMR spectroscopy, MALDI-TOF mass spectrometry, and elemental analysis [see the Supporting Information (SI)]. The molecular structure of **1**

**Received:** February 27, 2015
**Published:** May 14, 2015





DOI: 10.1021/jacs.5b02118
J. Am. Chem. Soc. 2015, 137, 6448–6451

in crystalline **1**·$CHCl_3$ was analyzed by single-crystal X-ray diffraction (Figure 1a), which confirmed a distorted square-planar coordination geometry around the nickel atom.

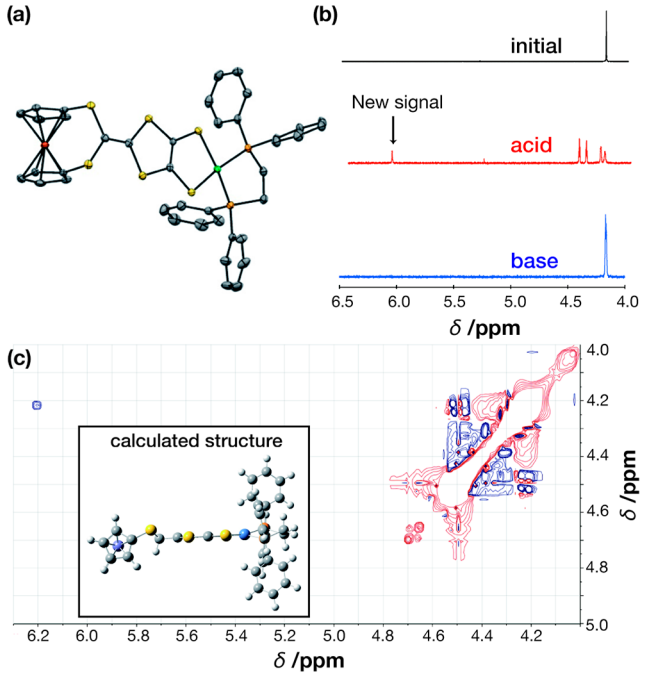


**Figure 1.** (a) ORTEP drawing of **1** with thermal ellipsoids at the 50% probability level. Hydrogen atoms have been omitted for clarity. (b) Changes in the $^1$H NMR spectrum upon acid/base addition to **1** in $CDCl_3$. (c) NOESY spectrum of [**1-H**]$^+$ in $CD_3CN$ and calculated structure of [**1-H**]$^+$.

The protonation behavior of **1** was investigated by $^1$H NMR spectroscopy. Figure 1b shows the changes in the spectrum upon acid/base addition to **1** in $CDCl_3$. When excess $CF_3SO_3H$ (acid) was added, the solution turned from green into purple, and a new proton signal appeared at $\delta$ = 6.15 ppm. Signal integration showed that the new peak corresponded to one proton, indicating that the monoprotonation was completed to form [Ni(dppe)($FcS_4$dt-H)]$^+$ ([**1-H**]$^+$) in this solution. Upon addition of excess NaOMe/MeOH (base), the peak at $\delta$ = 6.15 ppm disappeared and the initial signals appeared again, indicating that the protonation is reversible (eq 1). The reversibility was also confirmed by UV−vis spectroscopy (Figure S1a in the SI).

$$\mathbf{1} + H^+ \rightleftarrows [\mathbf{1\text{-}H}]^+ \quad (1)$$

The location of protonation was revealed by two-dimensional NMR spectroscopy in $CD_3CN$. The nuclear Overhauser effect spectroscopy (NOESY) spectrum of [**1-H**]$^+$ showed a clear correlation between the newly attached hydrogen atom at 6.20 ppm and the hydrogen atoms on the cyclopentadienyl (Cp) rings of the Fc moiety at 4.22 ppm (Figure 1c), indicating that these hydrogen atoms are sterically proximal to each other. Additionally, heteronuclear single-quantum coherence (HSQC) and $^{13}$C distortionless enhancement by polarization transfer (DEPT135) measurements showed that the carbon atom connected to the new hydrogen atom is tertiary (Figures S2−S4). These results suggest that the protonation occurs at the C=C bond of the dithiolene moiety, which agrees with our prediction (Scheme 1b). The protonation is accompanied by quasi-aromatization of the dithiafulvene ring, which stabilizes the resulting $\pi$-conjugated system.[8] The structure of [**1-H**]$^+$ is consistent with that calculated using density functional theory (DFT) (Figure 1c inset), in which the hydrogen newly attached is close (2.7 Å) to the two hydrogen atoms on the Cp rings. The protonation induces reconstruction of the $\pi$-conjugated structure with dramatic changes in the electrochemical and optical properties and the electronic structures, as discussed below.

Next, we conducted cyclic voltammetry (CV) of **1** and [**1-H**]$^+$ to determine how the protonation affects the intrinsic redox properties of **1**. Figure 2 shows cyclic voltammograms of

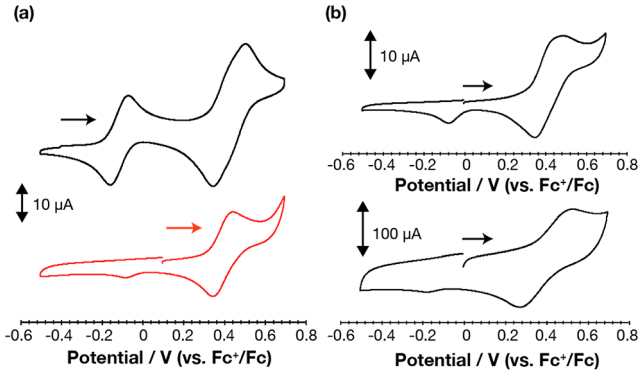


**Figure 2.** (a) Cyclic voltammograms of **1** (0.57 mM, black line) and [**1-H**]$^+$ (0.57 mM, red line) in $CH_2Cl_2$ containing 0.1 M $^t$Bu$_4$NPF$_6$ at a scan rate of 0.1 V s$^{-1}$. (b) Cyclic voltammograms of [**1-H**]$^+$ (0.57 mM) in $CH_2Cl_2$ containing 0.1 M $^t$Bu$_4$NPF$_6$ at scan rates of (top) 0.05 and (bottom) 3 V s$^{-1}$.

the complexes. **1** displayed a reversible oxidation wave at $E_1^{0\prime}$ = −0.14 V vs Fc$^+$/Fc and a quasi-reversible wave at a more positive potential with larger Faradaic currents. The first oxidation (eq 2) is attributed to the nickeladithiolene moiety

$$\mathbf{1} \rightleftarrows [\mathbf{1}]^{\bullet+} + e^- \quad (2)$$

on the basis of a comparison of $E_1^{0\prime}$ with those of reference nickeladithiolene complexes.[9] Therefore, the one-electron-oxidized form, [Ni(dppe)($FcS_4$dt)]$^{\bullet+}$ ([**1**]$^{\bullet+}$), is a $\pi$ radical in which the electron spin density is delocalized on the $\pi$-conjugated nickeladithiolene moiety. The $\pi$-radical character was confirmed by visible−near-infrared (vis−NIR) and electron spin resonance (ESR) spectroscopy. The second oxidation wave was considered to be a superposition of Fc-centered oxidation and a second oxidation centered on the nickeladithiolene moiety ($E_2^{0\prime}$ = 0.35 V and $E_3^{0\prime}$ = 0.46 V from the simulation in Figure S5).

[**1-H**]$^+$ exhibited the first oxidation wave at $E_1^{0\prime}$ = 0.35 V; this potential is similar to $E_2^{0\prime}$ and $E_3^{0\prime}$ of **1**, at which the Fc moiety was oxidized. This result is interpreted as follows. Protonation of **1** causes a shortened $\pi$-conjugation length with decreased numbers of $\pi$ electrons and quasi-aromatization with a positive charge on the nickeladithiolene skeleton, which modulates the characteristics of the nickeladithiolene-based orbitals. As a result, the Fc-based molecular orbital becomes the HOMO in [**1-H**]$^+$, and the first oxidation occurs mainly at the Fc moiety, forming [**1-H**]$^{\bullet2+}$ with a 3d spin on the Fc moiety (eq 3). This is in good agreement with the molecular orbitals calculated by DFT (Figure 3). Protonation greatly affects the frontier orbitals


DOI: 10.1021/jacs.5b02118
J. Am. Chem. Soc. 2015, 137, 6448−6451

$$[\mathbf{1\text{-}H}]^{+} \rightleftarrows [\mathbf{1\text{-}H}]^{\bullet 2+} + e^{-} \quad (3)$$

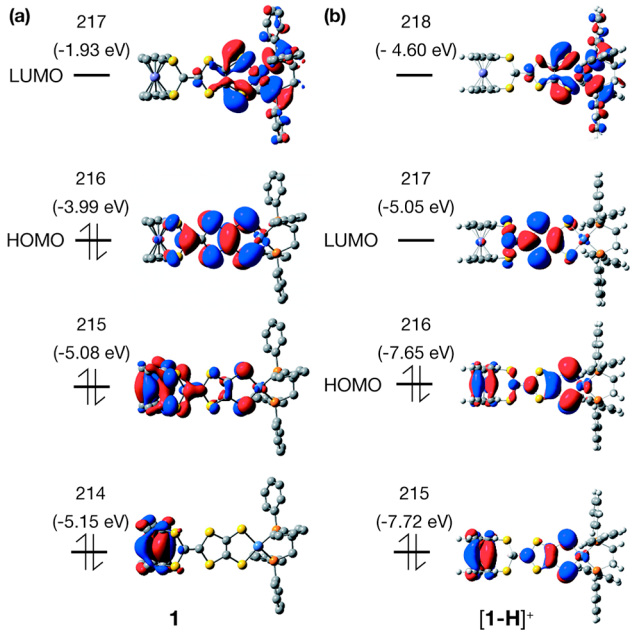


**Figure 3.** Calculated MOs for (a) **1** and (b) $[\mathbf{1\text{-}H}]^{+}$.

in **1** and $[\mathbf{1\text{-}H}]^{+}$. The HOMO is centered at the nickeladithiolene moiety in **1**, while it is distributed over the Fc moiety in $[\mathbf{1\text{-}H}]^{+}$.

The voltammogram of $[\mathbf{1\text{-}H}]^{+}$ (Figure 2a) shows a reduction peak current at $E_{pc1} = -0.13$ V corresponding to the reduction of the nickeladithiolene moiety after the anodic sweep. When the sweep rate was decreased, the peak current relative to the reduction peak current at $E_1^{0\prime} = 0.35$ V increased (Figures 2b and S5). These results indicate that the reversible protonation is coupled with the reversible redox ability, which can be rationalized as follows. $[\mathbf{1\text{-}H}]^{\bullet 2+}$ generated by the oxidation of $[\mathbf{1\text{-}H}]^{+}$ (eq 3) is unstable and is deprotonated to yield $[\mathbf{1}]^{\bullet +}$ and $H^{+}$ (eq 4) on a time scale comparable to the sweep rate of

$$[\mathbf{1\text{-}H}]^{\bullet 2+} \rightarrow [\mathbf{1}]^{\bullet +} + H^{+} \quad (4)$$

the CV measurements. The formation of $[\mathbf{1}]^{\bullet +}$ was confirmed by the appearance of the reduction peak current at $E_{pc1} = -0.13$ V. The dual-responsive nature of **1** allows the reaction shown in eq 3 to be followed by the reaction shown in eq 4. The deprotonation (eq 4) is expected to result in a drastic change in the spin density distribution on the molecule, as the Fc-centered 3d spin ($[\mathbf{1\text{-}H}]^{\bullet 2+}$) is transformed into the metal-ladithiolene-centered $\pi$ spin ($[\mathbf{1}]^{\bullet +}$). Next, we attempted to characterize $[\mathbf{1\text{-}H}]^{\bullet 2+}$ to determine whether the reactions shown above indeed proceed.

To characterize $[\mathbf{1\text{-}H}]^{\bullet 2+}$, the protonation and oxidation reactions shown in eqs 3 and 4 were monitored using vis−NIR spectroscopy at a low temperature (Figure 4a). The oxidant $[(4\text{-}BrC_6H_4)_3N][SbCl_6]$ (1 equiv) was added to a $CH_2Cl_2$ solution of $[\mathbf{1\text{-}H}]^{+}$ in the presence of $^{n}Bu_4NPF_6$ (4 equiv) at 233 K. $[\mathbf{1\text{-}H}]^{\bullet 2+}$ generated in situ displayed a weak absorption band at around 800 nm attributed to the ferrocenium moiety,[6c,10] indicating that the Fc moiety was oxidized in $[\mathbf{1\text{-}H}]^{\bullet 2+}$. When this reaction solution was heated to 293 K, the spectrum drastically changed to become nearly identical to that

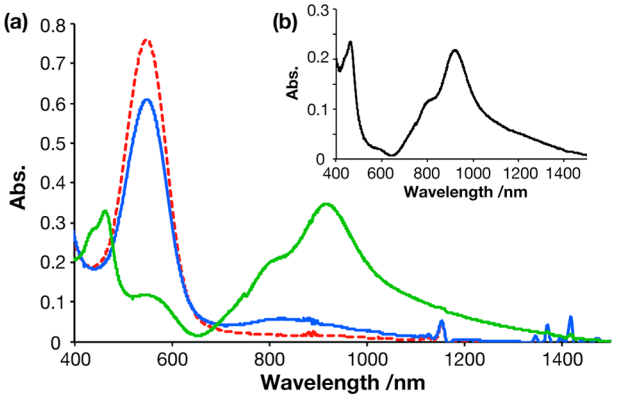


**Figure 4.** (a) Changes in the vis−NIR spectrum upon oxidation of $[\mathbf{1\text{-}H}]^{+}$: (red line) $[\mathbf{1\text{-}H}]^{+}$ at 233 K; (blue line) after addition of 1 equiv of the oxidant at 233 K; (green line) after heating to 293 K. (b) Vis−NIR spectrum of $[\mathbf{1}]^{\bullet +}$ at 293 K.

of $[\mathbf{1}]^{\bullet +}$ (Figure 4b). This change indicates that the deprotonation (eq 4) proceeded upon warming, thereby forming $[\mathbf{1}]^{\bullet +}$. This change was shown to be a single-step process from $[\mathbf{1\text{-}H}]^{\bullet 2+}$ to $[\mathbf{1}]^{\bullet +}$ by the time variation of the UV−vis−NIR spectra at 263 K (Figure S1b).[12]

The spin density distributions of the compounds and the reconstruction of the distribution upon deprotonation were directly observed by ESR spectroscopy. $[\mathbf{1}]^{\bullet +}$ in $CH_2Cl_2$ at 293 K showed a signal with $g_{iso} = 2.009$, confirming the $\pi$-radical character (Figure 5a). The splitting of the signal was caused by

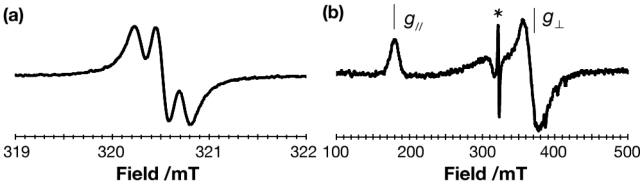


**Figure 5.** ESR spectra of (a) $[\mathbf{1}]^{\bullet +}$ at 293 K in $CH_2Cl_2$ solution and (b) $[\mathbf{1\text{-}H}]^{\bullet 2+}$ at 4.7 K in frozen $CH_2Cl_2$. The asterisk (*) indicates a signal derived from impurities.

hyperfine coupling with two phosphorus atoms ($A_P = 0.22$ mT).[11] In contrast, $[\mathbf{1\text{-}H}]^{\bullet 2+}$ in $CH_2Cl_2$, which was generated in situ by oxidizing $[\mathbf{1\text{-}H}]^{+}$ at 195 K in $CH_2Cl_2$ in the presence of $^{t}Bu_4NPF_6$, showed an axially anisotropic ESR signal at 4.7 K (Figure 5b). The obtained parameters ($g_{\parallel} = 3.58$, $g_{\perp} = 1.77$) and the spectral shape were characteristic of ferrocenium derivatives,[6c,13,14] suggesting that most of the electron spin density was localized on the Fe atom in the Fc moiety in $[\mathbf{1\text{-}H}]^{\bullet 2+}$. The ESR measurements on the $[\mathbf{1\text{-}H}]^{\bullet 2+}$ solution warmed to 293 K showed a spectrum that was changed drastically; the spectral parameters ($g_{iso} = 2.009$, $A_P = 0.22$ mT) were similar to those for $[\mathbf{1}]^{\bullet +}$ (Figure S6). These results indicate that $[\mathbf{1\text{-}H}]^{\bullet 2+}$ was converted to $[\mathbf{1}]^{\bullet +}$ by deprotonation upon warming. The deprotonation was accompanied by a large change in the spin density distribution of the molecule: the spin density moved from the Fc moiety (in $[\mathbf{1\text{-}H}]^{\bullet 2+}$) to the nickeladithiolene moiety (in $[\mathbf{1}]^{\bullet +}$). In other words, temperature-gated proton-coupled intramolecular electron transfer was observed, in which the temperature acted as the third external stimulus. Such a complex function controlled by multiple stimuli has rarely been reported in artificial molecular systems.


DOI: 10.1021/jacs.5b02118
J. Am. Chem. Soc. 2015, 137, 6448−6451

The results were fully consistent with the CV, DFT, and absorption spectroscopy results.

In conclusion, the proton−electron dual-responsive properties of **1** were investigated. The interplay of two stimuli-responsive properties generated two radical species with different spin characteristics ($\pi$ spin and 3d spin). The temperature-gated SR-PCET, the transformation from 3d spin to $\pi$ spin, was achieved in a single molecule. These findings show that the combination of protonation and electron transfer can be used to achieve complex functions within a single molecule that can be controlled by external stimuli.

## ■ ASSOCIATED CONTENT

### Supporting Information

Materials and methods, crystal structure data (CIF), spectral data, electrochemical data, and DFT calculation data. The Supporting Information is available free of charge on the ACS Publications website at DOI: 10.1021/jacs.5b02118.

## ■ AUTHOR INFORMATION


### Corresponding Authors

*kusamoto@chem.s.u-tokyo.ac.jp

*nisihara@chem.s.u-tokyo.ac.jp


### Notes

The authors declare no competing financial interest.

## ■ ACKNOWLEDGMENTS

We are grateful to Dr. Reizo Kato (RIKEN) for kind provision of facilities and laboratory equipment when our laboratory was under renovation. This work was supported financially by Grants-in-Aid from MEXT of Japan [26220801, 24750142, and 21108002; area 2107 (coordination programming)].

## ■ REFERENCES


(1) (a) Joachim, C.; Gimzewski, J.; Aviram, A. *Nature* **2000**, *408*, 541−548. (b) Whitesides, G. M.; Ismagilov, R. F. *Science* **1999**, *284*, 89−92. (c) Guldi, D. M.; Rahman, G. M. A.; Sgobba, V.; Ehli, C. *Chem. Soc. Rev.* **2006**, *35*, 471−487.

(2) (a) Huynh, M. H. V; Meyer, T. J. *Chem. Rev.* **2007**, *107*, 5004−5064. (b) Weinberg, D. R.; Gagliardi, C. J.; Hull, J. F.; Murphy, C. F.; Kent, C. A.; Westlake, B. C.; Paul, A.; Ess, D. H.; McCafferty, D. G.; Meyer, T. J. *Chem. Rev.* **2012**, *112*, 4016−4093.

(3) (a) Hirao, Y.; Saito, T.; Kurata, H.; Kubo, T. *Angew. Chem., Int. Ed.* **2015**, *54*, 2402−2405. (b) Ueda, A.; Yamada, S.; Isono, T.; Kamo, H.; Nakao, A.; Kumai, R.; Nakao, H.; Murakami, Y.; Yamamoto, K.; Nishio, Y.; Mori, H. *J. Am. Chem. Soc.* **2014**, *136*, 12184−12192. (c) Moore, G. F.; Hambourger, M.; Gervaldo, M.; Poluektov, O. G.; Rajh, T.; Gust, D.; Moore, T. A.; Moore, A. L. *J. Am. Chem. Soc.* **2008**, *130*, 10466−10467.

(4) (a) Sato, O.; Tao, J.; Zhang, Y.-Z. *Angew. Chem., Int. Ed.* **2007**, *46*, 2152−2187. (b) Tsukahara, N.; Minamitani, E.; Kim, Y.; Kawai, M.; Takagi, N. *J. Chem. Phys.* **2014**, *141*, No. 054702. (c) Liu, J.; Isshiki, H.; Katoh, K.; Morita, T.; Breedlove, B. K.; Yamashita, M.; Komeda, T. *J. Am. Chem. Soc.* **2013**, *135*, 651−658.

(5) (a) Kato, R. *Chem. Rev.* **2004**, *104*, 5319−5346. (b) Deplano, P.; Pilia, L.; Espa, D.; Mercuri, M. L.; Serpe, A. *Coord. Chem. Rev.* **2010**, *254*, 1434−1447.

(6) (a) Kusamoto, T.; Kume, S.; Nishihara, H. *J. Am. Chem. Soc.* **2008**, *130*, 13844−13845. (b) Kusamoto, T.; Kume, S.; Nishihara, H. *Angew. Chem., Int. Ed.* **2010**, *49*, 529−531. (c) Kusamoto, T.; Takada, K.; Sakamoto, R.; Kume, S.; Nishihara, H. *Inorg. Chem.* **2012**, *51*, 12102−12113.

(7) Li, X.-Y.; Sun, Y.-G.; Huo, P.; Shao, M.-Y.; Ji, S.-F.; Zhu, Q.-Y.; Dai, J. *Phys. Chem. Chem. Phys.* **2013**, *15*, 4016−4023.

(8) (a) Giffard, M.; Frere, P.; Gorgues, A.; Riou, A.; Roncali, J.; Toupet, L. *J. Chem. Soc., Chem. Commun.* **1993**, 944−945. (b) Giffard, M.; Alonso, P.; Garin, J.; Gorgues, A.; Nguyen, T. P.; Richomme, P.; Robert, A.; Ronculi, J.; Uriel, S. *Adv. Mater.* **1994**, *6*, 298−300.

(9) (a) Bowmaker, G. A.; Boyd, P. D. W.; Campbell, G. K. *Inorg. Chem.* **1983**, *22*, 1208−1213. (b) Vicente, R.; Ribas, J. *Inorg. Chim. Acta* **1981**, *132*, 229−236.

(10) Herring, F. G.; McLean, R. A. N. *Inorg. Chem.* **1972**, *11*, 1667−1669.

(11) Arumugam, K.; Shaw, M. C.; Mague, J. T.; Bill, E.; Sproules, S.; Donahue, J. P. *Inorg. Chem.* **2011**, *50*, 2995−3002.

(12) Figure S1b shows isosbestic points, suggesting that the change shown in eq 4 is a single-step process.

(13) Prins, R. *Mol. Phys.* **1970**, 603−620.

(14) Kusamoto, T.; Nishihara, H.; Kato, R. *Inorg. Chem.* **2013**, *52*, 13809−13811.




DOI: 10.1021/jacs.5b02118
*J. Am. Chem. Soc.* 2015, 137, 6448−6451